Development 135, 1179-1187 (2008) doi:10.1242/dev.010694

High-speed imaging of developing heart valves reveals interplay of morphogenesis and function

Paul J. Scherz, Jan Huisken, Pankaj Sahai-Hernandez and Didier Y. R. Stainier*

Knowing how mutations disrupt the interplay between atrioventricular valve (AVV) morphogenesis and function is crucial for understanding how congenital valve defects arise. Here, we use high-speed fluorescence microscopy to investigate AVV morphogenesis in zebrafish at cellular resolution. We find that valve leaflets form directly through a process of invagination, rather than first forming endocardial cushions. There are three phases of valve function in embryonic development. First, the atrioventricular canal (AVC) is closed by the mechanical action of the myocardium, rolls together and then relaxes. The growing valve leaflets serve to block the canal during the roll and, depending on the developmental stage, either expand or hang down as a leaflet to block the canal. These steps are disrupted by the subtle morphological changes that result from inhibiting ErbB-, TGFβ- or Cox2 (Ptgs2)-dependent signaling. Cox2 inhibition affects valve development due to its effect on myocardial cell size and shape, which changes the morphology of the ventricle and alters valve geometry. Thus, different signaling pathways regulate distinct aspects of the behavior of individual cells during valve morphogenesis, thereby influencing specific facets of valve function.

KEY WORDS: Cardiovascular development, Cox2 (Ptgs2), Microscopy, Prostaglandins, SPIM, Zebrafish

INTRODUCTION

The heart is the earliest functioning organ and is required soon after gastrulation, early in its own morphogenesis. Its function must change as its morphology changes: it first acts as a simple linear tube, then as two chambers separated by endocardial cushions, then, in higher vertebrates, as four chambers separated by valve leaflets (for reviews, see Glickman and Yelon, 2002; Olson, 2006). A defect at any of these transitions leads to swift embryonic death in amniotes, while minor congenital heart defects can lead to severe problems later in life. Thus, the cardiac developmental program is crucial for heart function and embryonic survival. Recent studies in zebrafish have revealed the flip side of this relationship: heart function is also required for cardiac morphogenesis (Hove et al., 2003; Bartman et al., 2004; Auman et al., 2007). For example, altering myocardial function can change myocardial cell shape (Auman et al., 2007).

The complex morphogenesis of the atrioventricular valve (AVV) is at the center of this relationship between form and function. During the linear heart tube phase, the heart may function as a suction pump (Forouhar et al., 2006) and does not require valves. As the heart loops, it becomes less efficient at preventing retrograde flow, causing the need for valves (Liebling et al., 2006). In mice and chicks, the extracellular matrix, or cardiac jelly, of the atrioventricular canal (AVC) swells, and its composition changes as the heart develops (reviewed by Armstrong and Bischoff, 2004). The atrioventricular endocardial cells undergo an epithelial-to-mesenchymal transition (EMT), migrate into the cardiac jelly and proliferate to form the endocardial cushions. These cushions are remodeled into mature valve leaflets. This process is controlled by many signaling pathways, including Notch (Timmerman et al., 2004), ErbB (Camenisch et al., 2002; Iwamoto et al., 2003), Bmp (Ma et al., 2005; Rivera-Feliciano and Tabin, 2006), TGFβ (Potts and Runyan, 1989), Wnt (Hurlstone et al., 2003) and NFAT (Chang et al., 2004). Mutations in genes encoding components of these pathways cause valve defects and retrograde blood flow from ventricle to atrium, which disrupts the unidirectional flow of blood, reduces cardiac output and leads to death. The specific roles these different pathways play in valve morphogenesis are largely unknown.

The zebrafish AVV has been reported to form in a similar fashion to that of higher vertebrates. By 48 hours postfertilization (hpf), the AVC is defined molecularly by expression of *versican*, *bmp4* and *notch1b* (Walsh and Stainier, 2001), and morphologically by the transformation of AVC endocardial cells from a squamous to a cuboidal morphology (Beis et al., 2005). Endocardial cells from the ventricular side of the AVC extend processes, migrate into the space between the endocardium and myocardium at 60 hpf, and form what appears to be an endocardial cushion in both the superior and inferior AVC by 96 hpf (Beis et al., 2005). These endocardial cushions are remodeled into the adult valve leaflets. This process requires Notch (Beis et al., 2005; Timmerman et al., 2004), NFAT (Chang et al., 2004), Wnt (Hurlstone et al., 2003) and ErbB (Goishi et al., 2003) signaling, as in the mouse. Zebrafish embryos are suitable for investigating this process because they are transparent, amenable to genetic manipulation, can survive with severe heart defects until late stages of development, getting oxygen by diffusion, and can be easily treated with chemical inhibitors of signaling pathways (Glickman and Yelon, 2002).

In this study, we used selective plane illumination microscopy (SPIM) to investigate the changing morphology and function of the developing valve in zebrafish embryos and larvae. SPIM allows high-speed fluorescence imaging and optical sectioning with deep penetration at cellular resolution (Huisken et al., 2004). This technology allowed us to visualize changes in valve morphology over developmental time and in various experimental conditions at cellular resolution. We first showed that the zebrafish AVV does not form through an intermediate stage of mesenchymal endocardial cushions as previously reported, but directly forms leaflets by a process of invagination. We next analyzed the changing function of

Department of Biochemistry and Biophysics, Programs in Developmental Biology, Genetics and Human Genetics, Cardiovascular Research Institute, University of California, San Francisco, San Francisco, CA 94158, USA.

*Author for correspondence (e-mail: dstainier@biochem.ucsf.edu)

Accepted 8 January 2008

the valve through development. The efficiency of the valve, as measured by the number of blood cells flowing backwards through the AVC during each valve closure, increases over developmental time. We also disrupted individual aspects of valve function with inhibitors of ErbB receptors, TGFβ receptors or Cyclooxygenase 2 [Cox2; also known as Prostaglandin-endoperoxide synthase 2 (Ptgs2)]. These experiments revealed a novel role for Cox2 in determining the geometry of the valve. Specifically, Cox2 plays a role in regulating myocardial cell shape upstream of prostaglandin F2α (PGF2α) and thromboxane A2 (TXA2).

MATERIALS AND METHODS

Zebrafish lines

Zebrafish were raised under standard conditions at 28°C (Westerfield, 2000). We used wild-type AB and the transgenic lines *Tg(flk1:EGFP)*^{s843} (Beis et al., 2005), *Tg(gata1:dsRed)*^{sd2} (Traver et al., 2003) and *Tg(myl7:HRAS-EGFP)*^{s883} (D'Amico et al., 2007).

Pharmacological treatment

Embryos were dechorionated and treated with a 4 mM stock of AG1478 (Calbiochem) diluted to 4 μM, a 3 mM stock of SB431542 (Sigma) diluted to 3 μM, a 5 mM stock of AL8810 (Cayman) diluted to 5 μM, and 10 mM stocks diluted to final concentrations of 25 μM for CAY10404, 40 μM for NS398, 100 μM for furegrelate, 10 μM for SQ29548, 10 μM for PGF2α, 15 μM for indomethacin and 10 μM for U46619 (Cayman), or 1% DMSO. Embryos were raised at 28°C until imaging or harvesting.

Microinjection

Embryos were injected at the 1-2-cell stage with 2-4 ng *thromboxane synthase* MO (5′-AGCTGCATGATGGGATCTGTCAATC-3′), then raised at 28°C until harvesting.

Selective plane illumination microscopy

Animals were embedded in 1% low melting agarose in plastic syringes and imaged in SPIM as described previously (Huisken et al., 2004) using a 20×/0.5 NA water dipping objective. Fluorescence was excited in the focal plane with 488 nm and 561 nm laser beams. Images were recorded on two synchronously triggered cameras (Andor). The frame rate ranged from 70 to 160 frames per second (fps) depending on the size of the region of interest. The two channels were merged using Matlab and saved as avi movies with a frame rate of 15 fps.

Confocal microscopy

Animals were embedded in 4% low melt agarose and cut into 200 μm sections with a Leica VT1000S vibratome. Where indicated, sections were incubated overnight with 1:75 rhodamine-phalloidin (Molecular Probes). Images were acquired with a Zeiss LSM5 Pascal confocal microscope.

Immunohistochemistry

We used mouse monoclonal antibodies zn8 (Zebrafish Stock Center and Hybridoma Bank) at 1:10, as previously described (Beis et al., 2005).

RT-PCR

At 48 hpf hearts were purified as previously described (Burns and MacRae, 2006) and total RNA was isolated with Trizol (Invitrogen). The following primers were used to amplify each gene: 5′-ATCTGAAACCCTACAC-ATCCTTCGC-3′ and 5′-AGACGTTTTGCTAAAGTTCGCCGTG-3′ for *cox1*, 5′-TACTCATCCTTTGAGGAGATGACAG-3′ and 5′-GACCTT-TTACAGCTCTGAACTCCGC-3′ for *cox2a*, 5′-TTTCACAACAGCCC-TGAACC-3′ and 5′-GTTGAAGGACTCAACCAAGC-3′ for *cox2b* (Ishikawa et al., 2007) and 5′-GCATTTTGATGTGGTCAACG-3′ and 5′-ACTTGGTGGGTTCAGTCCAG-3′ for *tbxas*. Thirty cycles of PCR were performed.

Cell shape analysis

Image stacks of ca. 70 planes of hearts were recorded on a Zeiss LSM 5 Pascal. Images and meta-information were imported from lsm-files into Matlab (Mathworks) using tiffread2c.m (F. Nedelec) and lsminfo.m (P. Li). Each stack was rotated in steps of 15 degrees about the *y*- and the *z*-axis. For each angle the sum projection along *z* was calculated for the front half of the stack and saved into a tif file. A dedicated Matlab program was used to display the projections, outline cells, annotate them and save all information. In each projection all cells with a basal surface that appeared orthogonal to the direction of projection were analyzed. An adaptive contour algorithm was used to precisely follow the labeled membrane. All relevant information, including cell number, region, area A, perimeter P and pixel size was saved to a text file. The circularity C was calculated C=P^2/(4πA). The information in this file was processed and the statistical analysis performed in Microsoft Excel.

RESULTS

Morphogenesis and function of wild-type zebrafish AVV

We started to examine AVV morphogenesis using *Tg(flk1:EGFP)*^{s843}, a line that marks endocardial and endothelial cells (Jin et al., 2005). To our surprise, SPIM imaging showed that by 76 hpf, what looked by confocal imaging of fixed tissue to be the superior endocardial cushion (Fig. 1A) was actually a valve leaflet (Fig. 1B and see Movie 1 in the supplementary material). This leaflet was clearly visible at 85 hpf (Fig. 1C,D and see Movie 2 in the supplementary material), and was composed of two layers: an outer layer of cuboidal cells and an inner layer of larger and rounder cells. The collapse of the heart upon fixation made it possible to misconstrue the leaflet as an endocardial cushion in previous studies. Only high-speed imaging of live samples allows one to see this dynamic structure. These data suggest that the zebrafish endocardium does not form mesenchymal cushions, but instead remains a single sheet of cells as it invaginates to directly form the AVV leaflet. To ensure that we were not missing a stage of

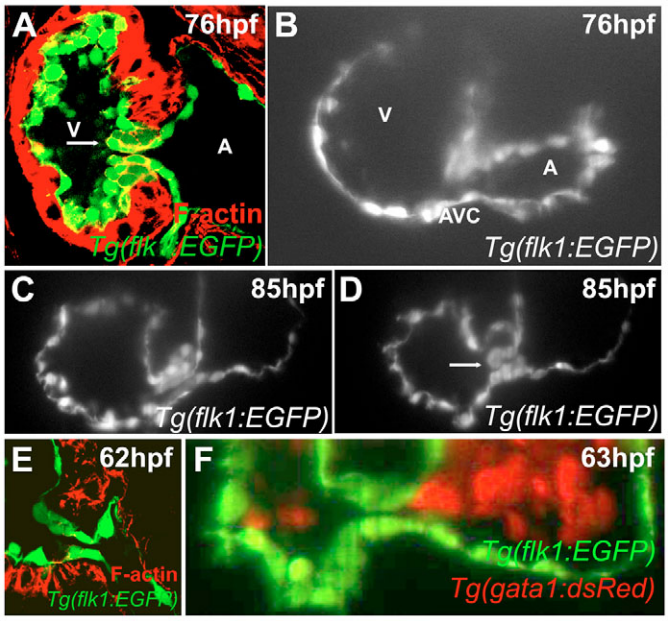

Fig. 1. Zebrafish valves form through invagination. Larvae were stained with rhodamine-phalloidin and imaged using confocal microscopy at 76 (**A**) or 62 (**E**) hpf, or imaged using SPIM at 76 (**B**), 85 (**C**,**D**) or 63 (**F**) hpf. Although by confocal microscopy a superior endocardial cushion appears to be present (panel A), SPIM imaging shows that this structure is actually a valve leaflet (B-D). Arrow in panel A points to the presumed endocardial cushion and that in D to the valve leaflet. No intermediate stage of mesenchymal cells was observed by either confocal (E) or SPIM imaging (F). A, atrium; V, ventricle.

mesenchymal cells that quickly resolved into a leaflet, we looked at stages between 56 and 72 hpf. At no stage did we observe mesenchymal cells in the AVC. For example, both confocal imaging at 62 hpf (Fig. 1E) and SPIM imaging at 63 hpf showed a sheet of connected cells (Fig. 1F and see Movie 3 in the supplementary material). Thus, zebrafish seem to have evolved a novel mechanism to form the AVV.

We next looked at how the function and efficiency of the valve leaflet change through development using a line carrying two transgenes, *Tg(flk1:EGFP)*^{s843} and *Tg(gata1:dsRed)*^{sd2} (Traver et al., 2003). The latter transgene marks blood cells, allowing visualization and quantification of blood flow through the AVC. At 55 hpf, before any cells had invaginated, the valve was not very efficient in preventing retrograde blood flow. The superior and inferior AVC were brought together mechanically by the action of myocardial contractions (Fig. 2A and see Movie 4 in the supplementary material). They then rolled together in an atrial-to-ventricular direction, almost touching one another (Fig. 2B). This roll prevented most retrograde blood flow, but the endocardium was not thick enough to fully occlude the AVC lumen, so some blood cells slipped back into the atrium. After the roll was complete, the AVC relaxed and opened, allowing many blood cells to flow backwards (Fig. 2C). Altogether, approximately ten cells flowed retrogradely from the time the superior and inferior AVC were brought together to the time the atrium contracted again (Fig. 2L, based on three embryos and 61 heartbeats).

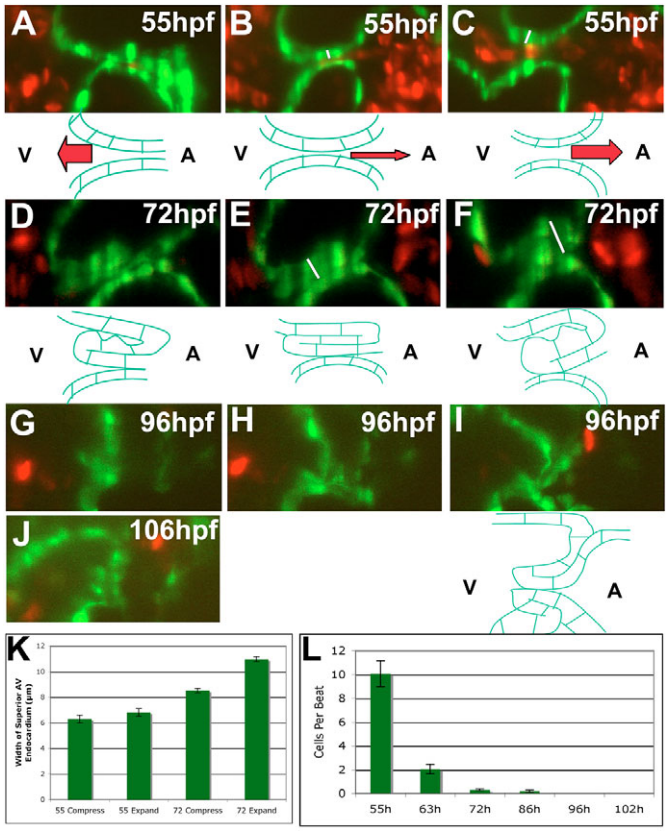

Fig. 2. Zebrafish AVV function becomes more efficient during development. Embryos and larvae were imaged using SPIM at 55 (**A-C**), 72 (**D-F**), 96 (**G-I**), and 106 (**J**) hpf. In 55 and 72 hpf animals, the thickness of the valves at the point of highest compression (i.e. white lines in B and E) and greatest expansion (i.e. white lines in C and F) was measured and the 95% confidence interval calculated (**K**). The number of cells flowing retrogradely across the AVC during valve function was counted for all stages along with the 95% confidence interval (**L**). (A-C) At 55 hpf, the AVC closes by the action of myocardial contractions (A), rolls atrially to ventricularly (B), and finally relaxes (C). The endocardium cannot occlude the lumen in these last two phases, leading to retrograde blood flow (B,C,L). (D-F) This three-part movement of the valve is repeated at 72 hpf, but a thick invaginating valve leaflet occludes the lumen during the roll and relaxation (E,F) through its compression and expansion (K). (G,H) The same three-part movement is found at 96 hpf, but the valve leaflet hangs down to occlude the lumen during relaxation (I). (J) By 106 hpf, both a superior and inferior valve leaflet are present. Drawings underneath the frames of the 55, 72 and last frame of the 96 hpf movies illustrate the shape of the AVC endocardial tissue in these pictures.

By 72 hpf, an average of three cells had invaginated at the deepest location. At this time point, there were not enough invaginated cells to hang down as a leaflet. Instead, they acted as a compressible mass of cells to occlude the AVC, perhaps similarly to the endocardial cushion of higher vertebrates. The AVC was still closed by the myocardial contractions: they brought together the two sides of the AVC (Fig. 2D and see Movie 5 in the supplementary material), which then rolled atrially to ventricularly (Fig. 2E). The valve structure was thick enough at this time to fully occlude the lumen through the roll. The invaginated cells were compressed as they were forced against the inferior wall of the AVC. Whereas at 55 hpf the AVC relaxed and opened at the end of the roll, at 72 hpf the valve structure expanded to occlude the AVC lumen (Fig. 2F). This compression and expansion can be quantified by measuring the width of the superior valve structure at its maximum compression during the roll and again at its maximum expansion during the relaxation (Fig. 2K, for examples of the width measured see white bars in B,C,E,F). At 55 hpf, there was no significant difference between the widths of the endocardium at these two time points (based on three embryos and 29 beats). By contrast, at 72 hpf, there was a significant difference between the width of the compressed and expanded valve structure (P<1.62E-25, based on three larvae and 30 beats). The thick, compressed tissue that blocked the lumen during the roll and the expanded tissue that occluded it during the relaxation phase combined to make the valve significantly more efficient at this stage than at 55 hpf, as measured by the number of blood cells undergoing retrograde flow: approximately 0.3 cells per beat at 72 hpf (Fig. 2L, P<2.03E-15, based on six larvae and 142 beats).

By 76 hpf, a valve leaflet was apparent in the superior AV endocardium (Fig. 1B), but its role in valve function could be most clearly seen at 96 hpf. In these samples, the sides of the AVC were still brought together by the myocardial contractions (Fig. 2G and see Movie 6 in the supplementary material). Even though a leaflet was present, the valve was not closed by hemodynamic forces. There was still the atrial-to-ventricular roll, with the thickness of the leaflet occluding the canal (Fig. 2H). The difference of this stage from 72 hpf was at the relaxation phase: instead of the tissue expanding to block the lumen of the AVC, the leaflet hung down to prevent retrograde blood flow (Fig. 2I). At this stage, the valve appeared to be 100% efficient, as we never observed any retrograde flow of blood cells (based on four samples and 113 heartbeats).

By 102 hpf, the valve was similar to the adult valve, in that both a superior and an inferior valve leaflet were present (Fig. 2J and see Movie 7 in the supplementary material). However, the AVC was still closed by the myocardial contractions instead of hemodynamic forces, and the rolling persisted. Both leaflets hung down across the AVC lumen to prevent retrograde flow.

Disrupting valve function

In this analysis, four main aspects of valve function stand out. First, the AVC closed by myocardial action. Next, the AVC rolled through the beat. Third, the valve tissue compressed and expanded to occlude the lumen during the relaxation phase. And finally, the valve structure increased in thickness to occlude the lumen during the roll. We tested the importance of these aspects for valve function and efficiency. Unfortunately, the first aspect could not be disrupted because it would lead to a complete loss of heart function. However, we identified chemical inhibitors that affected AVC rolling, valve compression and the increasing thickness of the endocardial tissue at the AVC.

ErbB signaling has been implicated in endocardial EMT in mouse (Camenisch et al., 2002; Iwamoto et al., 2003), as well as in valve function (Goishi et al., 2003) and AVC specification (Milan et al., 2006) in zebrafish. Because of the modified morphogenesis in zebrafish valve development, we wanted to investigate the role this signaling pathway might play in the process of invagination, and we used the ErbB receptor inhibitor AG-1478 (Goishi et al., 2003). We began treating embryos at 56 hpf, just before the invagination began, and imaged them with SPIM at 72 hpf. In the treated animals, the sides of the AVC were still brought together by the myocardial contractions, but because of a changed geometry of the invaginating tissue the AVC rolled in the reverse direction, i.e. ventricularly to atrially (Fig. 3A,B and see Movie 8 in the supplementary material). This altered roll resulted in the AVC lumen opening during the relaxation phase, allowing severe retrograde blood flow (Fig. 3C). The valve was significantly less efficient than wild type at the same stage, allowing the retrograde flow of approximately 8.6 cells per beat (Fig. 3F, $P<2.52E-11$, based on three larvae and 42 heartbeats). The subtly altered morphology of the valve was also apparent in confocal images of fixed tissues (Fig. 3E). The AVC endocardial cells did not fully invaginate and were separated from the cells on the outer surface of the leaflet by a space. These data suggest that the atrial-to-ventricular rolling is required for efficient valve function and that this mechanism plays a role in ensuring that the invaginated cells are in place for the relaxation phase.

We next studied inhibitors that block the compression and expansion of the valve. TGFβ signaling plays a role in endocardial EMT in amniotes (Potts and Runyan, 1989). As zebrafish valves form by a different mechanism, we wanted to investigate the potential role of TGFβ signaling in this process. Treating embryos with SB431542, an inhibitor of Alk4 (Acvr1b), 5 (Tgfbr1) and 7, from 56-72 hpf did not block endocardial invagination. However, in treated animals the invaginating cells retained a cuboidal appearance at 72 and 96 hpf in contrast to the large round cells seen in control larvae (Fig. 4A-D). The invaginating cells also failed to downregulate Alcam, an adhesion molecule expressed in the cuboidal cells on the outer surface of the leaflets (Fig. 4E,F) (Beis et al., 2005). Because these cells remained cuboidal, they appeared unable to compress and expand (see Movie 9 in the supplementary material). The thickness of the valve structure in treated larvae remained constant during all phases of the beat (Fig. 4G, based on three samples and 42 heartbeats). The valve in treated larvae had significantly decreased efficiency compared with control larvae at this stage, allowing the retrograde flow of approximately 1.9 cells per beat (Fig. 3F, $P<2.1E-27$, based on three samples and 124 heartbeats). Thus, it appears that compression and expansion of the valve tissue is important for valve function.

Next, we looked at the role of the increased thickness of the valve tissue during the rolling of the AVC. During a screen for chemical compounds that cause retrograde blood flow, we identified a number of Cox2 inhibitors. Treatment with two Cox2 inhibitors, NS-398 and CAY10404, from 56-72 hpf caused the invaginating structure to be shifted ventricularly (Fig. 5A-C and see Movie 10 in the supplementary material; data not shown). When the AVC closed and rolled, it was actually closing and rolling at a point where there was only a monolayer of endocardial cells (Fig. 5A,B). The valve structure only became involved at the end of the roll, the relaxation phase (Fig. 5C). Thus, for the initial part of the valve closure, the valve resembled the 55 hpf AVC, with no thick superior AV endocardium. As with the 55 hpf AVC, the endocardium in the treated larvae was unable to fully occlude the lumen, so many cells moved retrogradely, approximately three per beat, and the valve was significantly less efficient than control (Fig. 3F, $P<1.62E-14$, based on three larvae and 30 heartbeats). These data suggest that the thickening of the endocardium is important for valve function during the rolling phase.

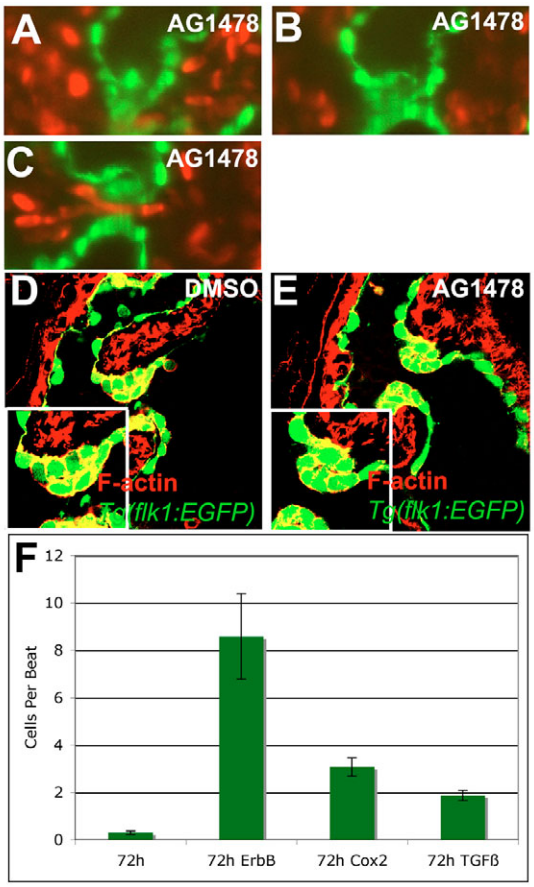

Fig. 3. Inhibiting ErbB signaling disrupted the rolling of the valve. Zebrafish embryos were treated with 4 μM AG1478, an ErbB receptor inhibitor, or 1% DMSO from 56-72 hpf and imaged with SPIM (**A-C**) or stained with rhodamine-phalloidin and imaged with confocal microscopy (**D**,**E**). Retrograde flow of blood cells per beat was quantified for animals treated with 1% DMSO, 4 μM AG1478, 25 μM CAY10404 or 3 μM SB431542 along with the 95% confidence interval (**F**). (A-C) Inhibition of ErbB signaling led to altered valve function, with the valve coming together on the ventricular side of the AVC (A), rolling ventricularly to atrially (B), and coming apart during the relaxation phase allowing retrograde blood flow (C,F). Larvae treated with inhibitor showed malformed valves with incomplete invagination and increased space between the two sides of the valve leaflet (E).

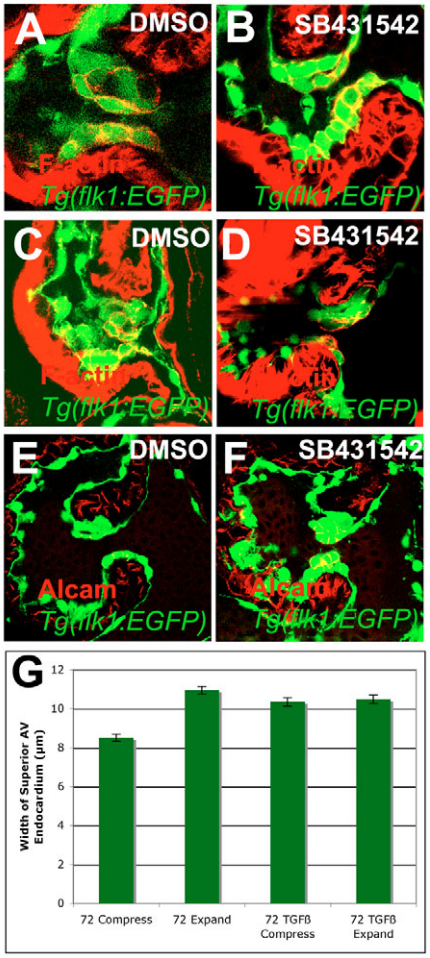

Fig. 4. Inhibition of TGFβ signaling disrupted the shape of invaginating valve cells. (**A-G**) Zebrafish embryos were treated with 1% DMSO (A,C,E) or 3 μM SB431542 (B,D,F) from either 56-72 (A,B,E,F) or 56-96 (C,D) hpf, and stained with rhodamine-phalloidin (A-D) or for Alcam (E,F) and imaged by confocal microscopy (A-F) or SPIM (G). The thickness of the valve at the point of greatest compression or expansion was measured and compared along with the 95% confidence interval (G). (A-D) Inhibition of TGFβ signaling resulted in cuboidal invaginating cells (B,D) compared with control valves (A,C). (E,F) TGFβ signaling was required for the downregulation of Alcam in the invaginating cells. (G) This change in shape and adhesion resulted in the inability of the valves to compress and expand.

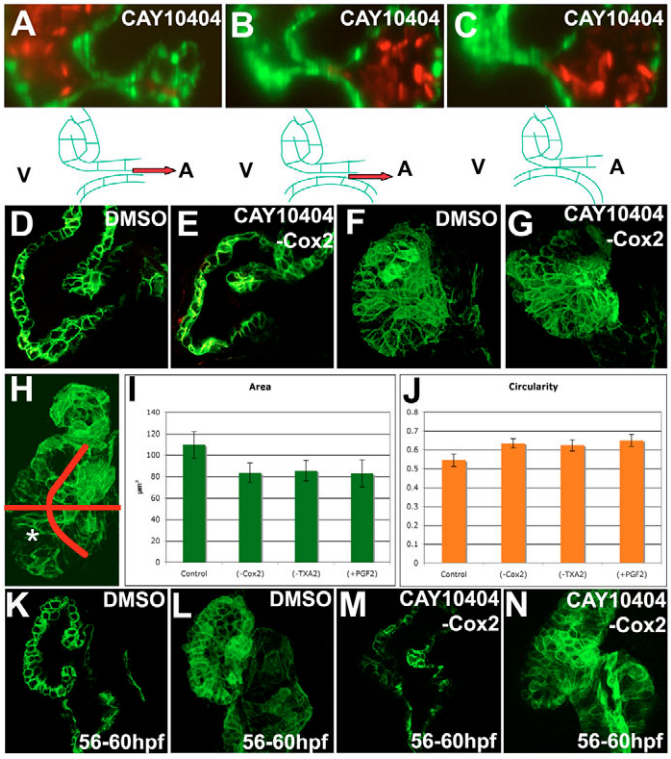

Fig. 5. Inhibition of Cox2 and prostaglandin signaling altered myocardial cell shape. Zebrafish embryos were treated with 25 μM CAY10404 (**A-C**,**E**,**G**,**M**,**N**), a Cox2 inhibitor, or 1% DMSO (**D**,**F**,**K**,**L**) from 56-72 (A-C,D-G) or 56-60 (K-N) hpf, imaged using SPIM (A-C) or confocal microscopy (D-G,K-N) and projections made (F,G,L,N). The area (**I**) and circularity (**J**) of cells in the posterior outer curvature of the ventricle was measured and the 95% confidence interval calculated. (A-C) Inhibition of Cox2 caused the invaginating cells to be translated towards the ventricle, such that the AVC closed (A) and rolled (B) on an endocardial monolayer leading to retrograde blood flow (B). (D,E) The invaginating cells shifted towards the ventricle because the myocardium overlying the superior AVC bent towards the ventricle (E). (F,G) This bending correlates with changes in ventricular shape caused by decreases in cell area (G,I) and increases in cell circularity (G,J). (**H**) The ventricle was divided into four areas based on anterior or posterior, outer or inner curvature, for the cell shape and circularity analysis. Significant differences were found in the posterior outer curvature of the ventricle, indicated with an asterisk. Myocardial bending (M) and cell shape changes (N) arose within 4 hours of treatment with Cox2 inhibitor.

Cox2 and myocardial cell shape

Why do Cox2 inhibitors cause invaginating cells to be translated towards the ventricle? When we looked at the myocardium using a myocardially expressed membrane-bound GFP in the *Tg(myl7:HRAS-EGFP)*^{s883} line (D'Amico et al., 2007), we found that the myocardium above the superior AVC bent inwards towards the ventricle in larvae treated with either of two Cox2 inhibitors, NS-398 or CAY10404 (Fig. 5E and data not shown). As the invaginating cells in these larvae were at the tip of this myocardium, they also moved towards the ventricle.

These findings raise the further question of why the myocardium overlying the AVC would bend. One possible explanation is that there are changes to myocardial cell shape in other parts of the ventricle. Auman et al. (Auman et al., 2007) recently showed that myocardial cells are larger and more elongated in the outer curvature of the ventricle than in the inner one. If cell shapes changed, then the shape of the whole ventricle might change. Analysis of 3D projections of hearts treated with Cox2 inhibitors suggested that cells in the posterior outer curvature were smaller and rounder than in control hearts (Fig. 5F,G). We measured myocardial cell shape using dedicated software that creates a 3D reconstruction of the heart based on confocal images and allows segmentation of myocardial cells and quantification of area and circularity (B. Jungblut, C. Munson, J.H., L. A. Trinh and D.Y.R.S., unpublished). Because there is an intrinsic difference between the outer and inner curvature of the ventricle, we analyzed these two areas separately. As we observed changes in the anterior inner curvature (the ventricle-wards bend) and the posterior outer curvature, we analyzed the anterior and posterior heart separately as well, giving four separate zones for analysis (Fig. 5H). Significant differences were observed only in the

posterior outer curvature, hence we focus our discussion on this area (Fig. 5H, asterisk). In animals treated with Cox2 inhibitors, there was a significant decrease in the cell surface area (P<0.0014) as well as a significant increase in the cell circularity (P<4.75E-5) (Fig. 5I,J, based on four samples and 48 cells for wild-type measurements and five samples and 81 cells for CAY10404-treated measurements). Thus, inhibition of Cox2 caused the cells of the posterior outer curvature of the ventricle to become smaller and rounder.

It is possible that altered flow at the AVC caused by the bending of the myocardium might lead to changes in myocardial cell shape, as in mutants with altered contraction and flow (Auman et al., 2007), rather than cell shape changes causing the bending. To determine which defect arises first, we performed timecourses of Cox2 inhibitor treatment. We found that myocardial bending and cell shape changes both arose 4 hours after initial treatment, either from 56-60 hpf (Fig. 5M,N) or 68-72 hpf (data not shown). We did not find one phenotype without the other. Although it is possible that changes in flow may swiftly lead to changes in myocardial shape, the close temporal relationship between the two defects supports a mechanism by which cell shape changes deform the ventricle, leading to the myocardial bending.

The balance of PGF2α and TXA2 signaling regulates myocardial cell shape

Cyclooxygenases transform the lipid arachidonic acid into prostaglandin H2 (PGH2) (see Fig. S1 in the supplementary material) (reviewed by Hata and Breyer, 2004; Cha et al., 2006b). PGH2 is the precursor used by prostanoid synthases to generate the five major prostaglandins produced in the embryonic zebrafish: prostaglandin E2 (PGE2), prostaglandin D2 (PGD2), PGF2α, prostacyclin and TXA2 (Cha et al., 2005; Yeh and Wang, 2006). These ligands bind to cell surface receptors and regulate a number of physiological and developmental processes, including, in zebrafish, gastrulation movements, vasculogenesis, renal patterning and hematopoietic stem cell homeostasis (Cha et al., 2005; Cha et al., 2006a; North et al., 2007). To identify the downstream effectors of Cox2 in the heart, we overexpressed or inhibited each of the downstream pathways. Manipulation of PGE2, PGD2 or prostacyclin signaling had no effect on heart function or myocardial bending and failed to rescue the Cox2 inhibition defect (data not shown). By contrast, inhibition of TXA2 synthase (Tbxas; also known as Tbxas1 – ZFIN) with furegrelate, or inhibition of the TXA2 (TP) receptor with SQ29548 caused the same bending of the AVC myocardium into the ventricle as in larvae treated with Cox2 inhibitors (Fig. 5A and data not shown). Similarly, the cells of the posterior outer curvature of the ventricle in SQ29548 treated larvae were significantly smaller (P<0.004) and rounder (P<0.000725) than in control larvae (Fig. 5I,J, Fig. 6B based on five samples and 59 cells).

To further test the role of Tbxas in this process, we used translation-blocking morpholinos (MO). Injection of 2 ng of MO led to pericardial edema at 48 and 72 hpf, with generally no other body defects (see Fig. S2 in the supplementary material; 114/140 (81%) from three injections). Injection of 4 ng caused pericardial edema and curving of the tail. Confocal microscopy revealed that the injected embryos exhibited the same myocardial cell shape changes (Fig. 6C,D) as those in which Tbxas, TP receptor or Cox2 had been inhibited. RT-PCR analysis revealed the expression of *tbxas*, *cox1* (*ptgs1*), *cox2a* and *cox2b* in isolated embryonic hearts (Fig. 6E).

Treatment with PGF2α beginning at 56 hpf had the same effect as inhibition of Cox2 or TXA2 signaling. The myocardium overlying the superior AVC bent towards the ventricle (Fig. 6F), and

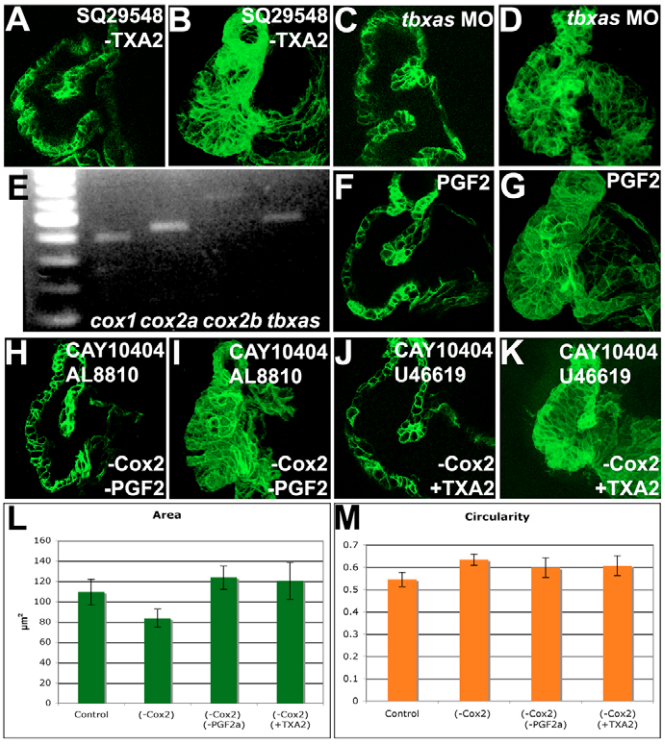

Fig. 6. Activation of TXA2 signaling or inhibition of PGF2α rescued the Cox2 inhibition phenotype. Zebrafish embryos were treated with 10 μM SQ29548 (**A**,**B**), a TP receptor inhibitor, 25 μM CAY10404 and 5 μM AL8810 (H,I), an FP receptor inhibitor, 25 μM CAY10404 and 10 μM U46619 (J,K), a TP receptor agonist, or injected with *tbxas* morpholinos (**C**,**D**), imaged with confocal microscopy (A-D,F-K), projections made (B,D,G,I,K) and the area (L) and circularity (M) measured and the 95% confidence interval calculated. Myocardial bending (A,C,F) and cell shape changes (B,D,G) were observed in larvae in which TXA2 signaling was inhibited (A-D) or PGF2α signaling was increased (**F**,**G**). (**E**) RT-PCR was performed on RNA from isolated hearts for *cox1*, *cox2a*, *cox2b* and *tbxas*. *cox1*, *cox2a*, *cox2b* and *tbxas* are expressed in the heart. (**H-M**) Inhibition of PGF2α signaling (H,I) or activation of TXA2 signaling (J,K) rescued the Cox2 inhibition phenotypes of myocardial bending (H,J) and the decrease in myocardial cell area (I,K,L), but not the increase in myocardial circularity (M).

the cells of the posterior outer curvature of the ventricle were smaller (P<0.0043) and rounder (P<2.79E-5) than in control larvae (Fig. 5I,J, Fig. 6G, based on three samples and 31 cells). These results suggest that PGF2α or TXA2 signaling may be perturbed when Cox2 is inhibited. Studies in mammals have shown an involvement of PGF2α and TXA2 in myocardial hypertrophy (Adams et al., 1996; Lai et al., 1996; Ponicke et al., 2000; Jovanovic et al., 2006); thus they are good candidates for pathways that affect myocardial cell shape.

If overactivation of PGF2α signaling or loss of TXA2 signaling is the result of Cox2 inhibition on valve formation, then the Cox2 inhibition phenotype should be rescued by treating with an inhibitor of PGF2α signaling or an activator of TXA2 signaling. Indeed, when we treated embryos with a Cox2 inhibitor and a PGF2α (FP) receptor inhibitor, the myocardium overlying the superior AVC did not bend and the cells of the posterior outer curvature of the ventricle were significantly larger than in larvae treated with a Cox2 inhibitor alone (P<6.3E-7), but not significantly different from control (Fig. 6H,I,L, based on three samples and 41 cells). The circularity of the

myocardial cells in the posterior outer curvature of the ventricle in these treated larvae was intermediate between that of Cox2 inhibitor-treated and control larvae, but these differences were not significant (Fig. 6M). Thus it appears that inhibiting PGF2α signaling can rescue all the phenotypes due to Cox2 inhibition, except the increased circularity of myocardial cells.

Similarly, treating with an agonist of the TP receptor, U46619, at the same time as a Cox2 inhibitor rescued the Cox2 inhibition phenotype. The myocardium overlying the superior AVC did not bend ventricularly (Fig. 6J). Cells of the posterior outer curvature of the ventricle were significantly larger than in Cox2 inhibited larvae (P<0.0012), but not significantly different in size from control larvae (Fig. 6K,M, based on two samples and 23 cells). However, again we did not rescue the circularity of these cells (Fig. 6F). They were significantly more circular than in control larvae (P<0.034), but not significantly different from in the Cox2-inhibited larvae.

These data suggest that the balance between PGF2α and TXA2 signaling regulates myocardial cell shape in the developing heart. In other systems of prostanoid signaling, the balance between different pathways is crucial. For example, prostacyclin causes vasodilation and inhibits platelet clotting whereas TXA2 causes vasoconstriction and promotes platelet clotting (McAdam et al., 1999; Cheng et al., 2002; Egan et al., 2004; Fitzgerald, 2004). If prostacyclin signaling is lost, then excess TXA2 signaling causes thrombotic events. If such a balance is important in regulating myocardial cell shape, then inhibiting the FP receptor should rescue the TP receptor inhibition phenotype. Indeed, larvae treated with both inhibitors did not have a bent myocardium and the cells were significantly larger than in larvae treated with the TP receptor inhibitor alone (Fig. 7A,B,E, P<1.65E-5, based on four larvae and 38 cells). Again, the circularity of the cells was not rescued, as the double-treated larvae had cells that were significantly more circular than controls (Fig. 6F, P<0.02).

Thus it seems that the PGF2α and TXA2 pathways at least partially antagonize each other with regard to myocardial cell size. It is clear how Cox2 might be required for TXA2 signaling by providing the PGH2 precursor in cells producing TXA2 (see Fig. S1 in the supplementary material). Previous studies in adult rodent hearts show that Cox2 activity can give rise to TXA2 production (Grandel et al., 2000; Zhang et al., 2003). The question remains how inhibiting Cox2 might produce an excess of PGF2α signaling. One possibility is that Cox1 alone can provide the precursor for PGF2α production, whereas Cox2 provides the precursor for TXA2 production (Fig. 7G). Inhibition of Cox2 would remove TXA2, but Cox1 would continue producing PGH2 for PGF2α. Therefore the relative balance of the two would be skewed in favor of PGF2α signaling. One can test this hypothesis by inhibiting both Cox1 and Cox2. If this hypothesis is correct, then treated larvae should not show the Cox2 phenotype but have a phenotype akin to that of the larvae treated with both the TP and FP receptor inhibitors. We treated

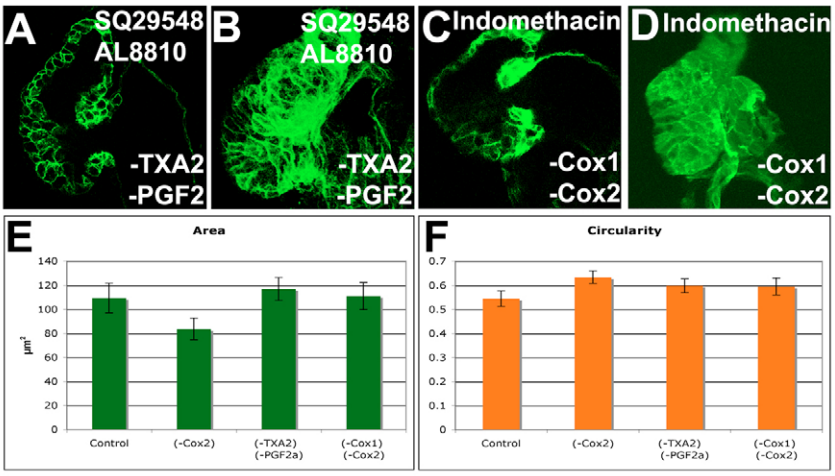

G

	Superior AVC Myocardium	Myocardial Cell Area	Myocardial Cell Circularity
-Cox-2	Bent	Decreased	Increased
-TXA2	Bent	Decreased	Increased
+PGF2α	Bent	Decreased	Increased
-Cox-2 - PGF2α	Wildtype	Wildtype	Slightly Increased
-Cox-2 +TXA2	Wildtype	Wildtype	Slightly Increased
-TXA2 - PGF2α	Wildtype	Wildtype	Slightly Increased
-Cox-1 -Cox-2	Wildtype	Wildtype	Slightly Increased

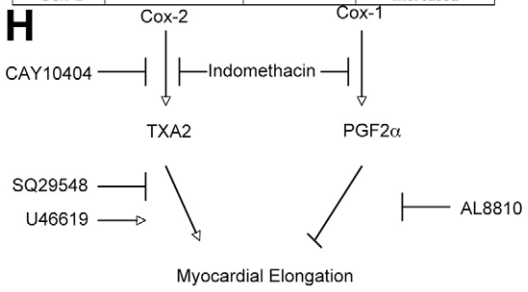

Fig. 7. A balance of TXA2 and PGF2α signaling regulates myocardial cell shape. Zebrafish embryos were treated with 10 μM SQ29548 and 5 μM AL8810 (**A**,**B**), or 15 μM indomethacin (**C**,**D**), an inhibitor of Cox1 and Cox2, imaged with confocal (A-D), projections made (B,D) and the area (**E**) and circularity (**F**) measured and the 95% confidence interval calculated. Inhibition of both PGF2α and TXA2 signaling (A,B) or all Cox signaling (C,D) gave wild-type shape of the myocardium overlying the AVC (A,C) and wild-type myocardial area (B,D,E), although myocardial circularity was increased (F). (**G**) Table of the effects of inhibiting or activating different signaling pathways. (**H**) These findings suggest a model in which Cox2-derived TXA2 supports myocardial elongation, whereas PGF2α arising from Cox1 action or from the action of both Cox1 and Cox2 inhibits myocardial elongation.

embryos with indomethacin, which inhibits both Cox1 and Cox2. As predicted, the larvae were phenotypically similar to the TP- and FP-receptor-inhibited larvae. The myocardium did not bend towards the ventricle, and the cells were significantly larger than in Cox2-inhibited larvae ($P<0.00033$), but not significantly different in area from controls (Fig. 7C-E, based on four larvae and 45 cells). These cells were significantly more circular than controls (Fig. 6F, $P<0.04$). Thus, inhibiting Cox1 partially rescues Cox2 inhibition in a way similar to FP receptor inhibition. This finding suggests that Cox1 activity may be responsible for the continued PGF2α signaling in Cox2-inhibited animals.

DISCUSSION

In this paper, we have presented several findings regarding zebrafish AVV morphogenesis and function. Importantly, unlike in mice or chickens, zebrafish atrioventricular endocardial cells do not appear to give rise to mesenchymal cushions. This finding illustrates the necessity of high-speed fluorescence microscopy of live embryos in contrast to fixed, and possibly deformed, tissues. The AVC endocardium extends processes into the space between the endocardium and myocardium and invaginates, beginning at the ventricular side of the AVC, to directly form a valve leaflet. We call it an invagination because the cells appear to remain in a sheet throughout the process. In addition to cell movements, there is a downregulation of the adhesion molecule Alcam and a change in cell shape from cuboidal to large, round cells (Beis et al., 2005). Based on our results, TGFβ signaling seems to regulate these processes. The development of antibodies and new transgenic lines that allow the examination of subcellular structures during invagination will be required to determine how closely this process resembles EMT.

Why is this process so different from that in mouse and chick? One possible explanation is that this invagination is the more basal mechanism for valve development, with large mesenchymal cushions arising in tetrapods due to the demands of the more complicated, septated hearts of higher vertebrates. However, this explanation does not seem to hold true, as histological analyses of the hearts of both the dogfish (Gallego et al., 1997), a chondrichthyan, and the sturgeon (Icardo et al., 2004), a more basal fish than zebrafish, show mesenchymal cushions, suggesting that the mechanism of forming mesenchymal cushions by EMT is more ancient than simple invagination. An alternative explanation is that invagination is a novel mechanism that evolved at some point in the zebrafish lineage since its divergence from sturgeon. Perhaps because of the small size of its embryonic heart, zebrafish bypassed a complicated and apparently unnecessary step of valve development.

Interestingly, the invagination process still requires the signaling pathways that are necessary for the development of endocardial cushions in mice and chicks. Notch, NFAT, ErbB and TGFβ signaling are all required in zebrafish valve development. They have been harnessed for a seemingly different process. Our understanding of the role of these pathways at the level of the individual cell is relatively poor because of the lack of readouts in higher vertebrates. The phenotypes of EMT mouse mutants are basically bimodal: either EMT occurs or it does not. In vitro explants allow a greater degree of discrimination, but it is difficult to know how closely in vitro systems parallel the in vivo situation. Although the overall process of valve formation is different in zebrafish and amniotes, at the level of the single cell a signaling pathway may be functioning in similar ways. Thus, investigations into how these pathways regulate zebrafish valve development may shed light on their specific function in higher vertebrates. Importantly, though, these results suggest the need for care in making comparisons among the species and the need to look more carefully into the exact effects of experimental manipulations.

In this study, we have also analyzed how valve function changes throughout the development of the AVV leaflets. Function improves with the changing morphology, but some aspects remain the same. For example, at all stages examined, the two sides of the AVC were brought together mechanically by the action of myocardial contraction. Again, at all stages, the AVC rolled together in an atrial-to-ventricular direction, and if this movement was disrupted, retrograde blood flow resulted.

Our results suggest that the most important changes are the two ways in which the developing leaflets function to better occlude the lumen and prevent retrograde blood flow. First, the growing thickness of the developing leaflet alone helped to block off the AVC during the rolling motion. Second, the developing leaflet blocked the lumen after the roll was over and the valve relaxed. At earlier stages it achieved this task simply by expanding. This function of the forming leaflet may be similar to that of the mesenchymal cushions in other vertebrates. Although structurally distinct (mesenchyme with an overlying endothelium versus endothelium elaborated into the beginnings of a leaflet), at a functional level they are similar, a compressible mass of cells. At later stages, the leaflet hung down to block the AVC lumen. Again, valve function at this stage could be similar to that in higher vertebrates when the endocardial cushions remodel into valve leaflets. These observations support the results of Liebling et al. (Liebling et al., 2006), who observed that after the initial inefficiency of the looped heart, the heart becomes more efficient, and prevents all retrograde flow by 96-111 hpf.

In our attempts to alter valve function, we made another significant finding: the importance of Cox2-dependent myocardial cell shape changes for AVV function. Our results suggest that Cox2 is required to control the balance between PGF2α and TXA2 signaling in the heart. This balance ensures the elongation of myocardial cells in the posterior outer curvature of the ventricle. Studies in mice have shown a function for these pathways in myocardial hypertrophy. It will be important to study whether there is any resemblance between the embryonic and adult mechanism of prostanoid-dependent cell shape changes, as well as the effect of these inhibitors on adult hearts.

Together, these disruptions of valve morphogenesis indicate the complex nature of heart development, a process that can only be fully evaluated by careful high-speed SPIM analyses. The results herein illustrate how subtle alterations in cell shape and movement caused by inhibition of distinct signaling pathways can lead to severe disruptions in heart function.

We thank the members of the Stainier lab, especially B. Jungblut and P. Aanstad for helpful advice. We thank S. Morton, J. Williams and B. Wolff for their assistance and advice. P.J.S. was supported by a postdoctoral fellowship from the Helen Hay Whitney Foundation. J.H. was supported by a postdoctoral fellowship from the Human Frontier Science Program Organization. P.S.-H. was supported by a summer undergraduate research fellowship from the NSF. This work was funded in part by grants from the NIH (NHLBI) and the Packard Foundation to D.Y.R.S.

Supplementary material

Supplementary material for this article is available at http://dev.biologists.org/cgi/content/full/135/6/1179/DC1

References

Adams, J. W., Migita, D. S., Yu, M. K., Young, R., Hellickson, M. S., Castro-Vargas, F. E., Domingo, J. D., Lee, P. H., Bui, J. S. and Henderson, S. A.

(1996). Prostaglandin F2 alpha stimulates hypertrophic growth of cultured neonatal rat ventricular myocytes. *J. Biol. Chem.* **271**, 1179-1186.
Armstrong, E. J. and Bischoff, J. (2004). Heart valve development: endothelial cell signaling and differentiation. *Circ. Res.* **95**, 459-470.
Auman, H. J., Coleman, H., Riley, H. E., Olale, F., Tsai, H. J. and Yelon, D. (2007). Functional modulation of cardiac form through regionally confined cell shape changes. *PLoS Biol.* **5**, e53.
Bartman, T., Walsh, E. C., Wen, K. K., McKane, M., Ren, J., Alexander, J., Rubenstein, P. A. and Stainier, D. Y. (2004). Early myocardial function affects endocardial cushion development in zebrafish. *PLoS Biol.* **2**, E129.
Beis, D., Bartman, T., Jin, S. W., Scott, I. C., D'Amico, L. A., Ober, E. A., Verkade, H., Frantsve, J., Field, H. A., Wehman, A. et al. (2005). Genetic and cellular analyses of zebrafish atrioventricular cushion and valve development. *Development* **132**, 4193-4204.
Burns, C. G. and MacRae, C. A. (2006). Purification of hearts from zebrafish embryos. *Biotechniques* **40**, 274, 276, 278 passim.
Camenisch, T. D., Schroeder, J. A., Bradley, J., Klewer, S. E. and McDonald, J. A. (2002). Heart-valve mesenchyme formation is dependent on hyaluronan-augmented activation of ErbB2-ErbB3 receptors. *Nat. Med.* **8**, 850-855.
Cha, Y. I., Kim, S. H., Solnica-Krezel, L. and Dubois, R. N. (2005). Cyclooxygenase-1 signaling is required for vascular tube formation during development. *Dev. Biol.* **282**, 274-283.
Cha, Y. I., Kim, S. H., Sepich, D., Buchanan, F. G., Solnica-Krezel, L. and DuBois, R. N. (2006a). Cyclooxygenase-1-derived PGE2 promotes cell motility via the G-protein-coupled EP4 receptor during vertebrate gastrulation. *Genes Dev.* **20**, 77-86.
Cha, Y. I., Solnica-Krezel, L. and DuBois, R. N. (2006b). Fishing for prostanoids: deciphering the developmental functions of cyclooxygenase-derived prostaglandins. *Dev. Biol.* **289**, 263-272.
Chang, C. P., Neilson, J. R., Bayle, J. H., Gestwicki, J. E., Kuo, A., Stankunas, K., Graef, I. A. and Crabtree, G. R. (2004). A field of myocardial-endocardial NFAT signaling underlies heart valve morphogenesis. *Cell* **118**, 649-663.
Cheng, Y., Austin, S. C., Rocca, B., Koller, B. H., Coffman, T. M., Grosser, T., Lawson, J. A. and FitzGerald, G. A. (2002). Role of prostacyclin in the cardiovascular response to thromboxane A2. *Science* **296**, 539-541.
D'Amico, L., Scott, I. C., Jungblut, B. and Stainier, D. Y. (2007). A mutation in zebrafish hmgcr1b reveals a role for isoprenoids in vertebrate heart-tube formation. *Curr. Biol.* **17**, 252-259.
Egan, K. M., Lawson, J. A., Fries, S., Koller, B., Rader, D. J., Smyth, E. M. and Fitzgerald, G. A. (2004). COX-2-derived prostacyclin confers atheroprotection on female mice. *Science* **306**, 1954-1957.
Fitzgerald, G. A. (2004). Coxibs and cardiovascular disease. *N. Engl. J. Med.* **351**, 1709-1711.
Forouhar, A. S., Liebling, M., Hickerson, A., Nasiraei-Moghaddam, A., Tsai, H. J., Hove, J. R., Fraser, S. E., Dickinson, M. E. and Gharib, M. (2006). The embryonic vertebrate heart tube is a dynamic suction pump. *Science* **312**, 751-753.
Gallego, A., Duran, A. C., De Andres, A. V., Navarro, P. and Munoz-Chapuli, R. (1997). Anatomy and development of the sinoatrial valves in the dogfish (Scyliorhinus canicula). *Anat. Rec.* **248**, 224-232.
Glickman, N. S. and Yelon, D. (2002). Cardiac development in zebrafish: coordination of form and function. *Semin. Cell Dev. Biol.* **13**, 507-513.
Goishi, K., Lee, P., Davidson, A. J., Nishi, E., Zon, L. I. and Klagsbrun, M. (2003). Inhibition of zebrafish epidermal growth factor receptor activity results in cardiovascular defects. *Mech. Dev.* **120**, 811-822.
Grandel, U., Fink, L., Blum, A., Heep, M., Buerke, M., Kraemer, H. J., Mayer, K., Bohle, R. M., Seeger, W., Grimminger, F. et al. (2000). Endotoxin-induced myocardial tumor necrosis factor-alpha synthesis depresses contractility of isolated rat hearts: evidence for a role of sphingosine and cyclooxygenase-2-derived thromboxane production. *Circulation* **102**, 2758-2764.
Hata, A. N. and Breyer, R. M. (2004). Pharmacology and signaling of prostaglandin receptors: multiple roles in inflammation and immune modulation. *Pharmacol. Ther.* **103**, 147-166.
Hove, J. R., Koster, R. W., Forouhar, A. S., Acevedo-Bolton, G., Fraser, S. E. and Gharib, M. (2003). Intracardiac fluid forces are an essential epigenetic factor for embryonic cardiogenesis. *Nature* **421**, 172-177.
Huisken, J., Swoger, J., Del Bene, F., Wittbrodt, J. and Stelzer, E. H. (2004). Optical sectioning deep inside live embryos by selective plane illumination microscopy. *Science* **305**, 1007-1009.
Hurlstone, A. F., Haramis, A. P., Wienholds, E., Begthel, H., Korving, J., Van Eeden, F., Cuppen, E., Zivkovic, D., Plasterk, R. H. and Clevers, H. (2003). The Wnt/beta-catenin pathway regulates cardiac valve formation. *Nature* **425**, 633-637.
Icardo, J. M., Guerrero, A., Duran, A. C., Domezain, A., Colvee, E. and Sans-Coma, V. (2004). The development of the sturgeon heart. *Anat. Embryol.* **208**, 439-449.
Ishikawa, T. O., Griffin, K. J., Banerjee, U. and Herschman, H. R. (2007). The zebrafish genome contains two inducible, functional cyclooxygenase-2 genes. *Biochem. Biophys. Res. Commun.* **352**, 181-187.
Iwamoto, R., Yamazaki, S., Asakura, M., Takashima, S., Hasuwa, H., Miyado, K., Adachi, S., Kitakaze, M., Hashimoto, K., Raab, G. et al. (2003). Heparin-binding EGF-like growth factor and ErbB signaling is essential for heart function. *Proc. Natl. Acad. Sci. USA* **100**, 3221-3226.
Jin, S. W., Beis, D., Mitchell, T., Chen, J. N. and Stainier, D. Y. (2005). Cellular and molecular analyses of vascular tube and lumen formation in zebrafish. *Development* **132**, 5199-5209.
Jovanovic, N., Pavlovic, M., Mircevski, V., Du, Q. and Jovanovic, A. (2006). An unexpected negative inotropic effect of prostaglandin F2alpha in the rat heart. *Prostaglandins Other Lipid Mediat.* **80**, 110-119.
Lai, J., Jin, H., Yang, R., Winer, J., Li, W., Yen, R., King, K. L., Zeigler, F., Ko, A., Cheng, J. et al. (1996). Prostaglandin F2 alpha induces cardiac myocyte hypertrophy in vitro and cardiac growth in vivo. *Am. J. Physiol.* **271**, H2197-H2208.
Liebling, M., Forouhar, A. S., Wolleschensky, R., Zimmermann, B., Ankerhold, R., Fraser, S. E., Gharib, M. and Dickinson, M. E. (2006). Rapid three-dimensional imaging and analysis of the beating embryonic heart reveals functional changes during development. *Dev. Dyn.* **235**, 2940-2948.
Ma, L., Lu, M. F., Schwartz, R. J. and Martin, J. F. (2005). Bmp2 is essential for cardiac cushion epithelial-mesenchymal transition and myocardial patterning. *Development* **132**, 5601-5611.
McAdam, B. F., Catella-Lawson, F., Mardini, I. A., Kapoor, S., Lawson, J. A. and FitzGerald, G. A. (1999). Systemic biosynthesis of prostacyclin by cyclooxygenase (COX)-2: the human pharmacology of a selective inhibitor of COX-2. *Proc. Natl. Acad. Sci. USA* **96**, 272-277.
Milan, D. J., Giokas, A. C., Serluca, F. C., Peterson, R. T. and MacRae, C. A. (2006). Notch1b and neuregulin are required for specification of central cardiac conduction tissue. *Development* **133**, 1125-1132.
North, T. E., Goessling, W., Walkley, C. R., Lengerke, C., Kopani, K. R., Lord, A. M., Weber, G. J., Bowman, T. V., Jang, I. H., Grosser, T. et al. (2007). Prostaglandin E2 regulates vertebrate haematopoietic stem cell homeostasis. *Nature* **447**, 1007-1011.
Olson, E. N. (2006). Gene regulatory networks in the evolution and development of the heart. *Science* **313**, 1922-1927.
Ponicke, K., Giessler, C., Grapow, M., Heinroth-Hoffmann, I., Becker, K., Osten, B. and Brodde, O. E. (2000). FP-receptor mediated trophic effects of prostanoids in rat ventricular cardiomyocytes. *Br. J. Pharmacol.* **129**, 1723-1731.
Potts, J. D. and Runyan, R. B. (1989). Epithelial-mesenchymal cell transformation in the embryonic heart can be mediated, in part, by transforming growth factor beta. *Dev. Biol.* **134**, 392-401.
Rivera-Feliciano, J. and Tabin, C. J. (2006). Bmp2 instructs cardiac progenitors to form the heart-valve-inducing field. *Dev. Biol.* **295**, 580-588.
Timmerman, L. A., Grego-Bessa, J., Raya, A., Bertran, E., Perez-Pomares, J. M., Diez, J., Aranda, S., Palomo, S., McCormick, F., Izpisua-Belmonte, J. C. et al. (2004). Notch promotes epithelial-mesenchymal transition during cardiac development and oncogenic transformation. *Genes Dev.* **18**, 99-115.
Traver, D., Paw, B. H., Poss, K. D., Penberthy, W. T., Lin, S. and Zon, L. I. (2003). Transplantation and in vivo imaging of multilineage engraftment in zebrafish bloodless mutants. *Nat. Immunol.* **4**, 1238-1246.
Walsh, E. C. and Stainier, D. Y. (2001). UDP-glucose dehydrogenase required for cardiac valve formation in zebrafish. *Science* **293**, 1670-1673.
Westerfield, M. (2000). *The Zebrafish Book. A Guide for the Laboratory use of Zebrafish* (*Danio rerio*). Eugene: University of Oregon Press.
Yeh, H. C. and Wang, L. H. (2006). Profiling of prostanoids in zebrafish embryonic development. *Prostaglandins Leukot. Essent. Fatty Acids* **75**, 397-402.
Zhang, Z., Vezza, R., Plappert, T., McNamara, P., Lawson, J. A., Austin, S., Pratico, D., Sutton, M. S. and FitzGerald, G. A. (2003). COX-2-dependent cardiac failure in Gh/tTG transgenic mice. *Circ. Res.* **92**, 1153-1161.